

## Redirecting Coronavirus to a Nonnative Receptor through a Virus-Encoded Targeting Adapter

M. H. Verheije,<sup>1,2,†</sup> T. Würdinger,<sup>1,2,†</sup> V. W. van Beusechem,<sup>2</sup> C. A. M. de Haan,<sup>1</sup>  
W. R. Gerritsen,<sup>2</sup> and P. J. M. Rottier<sup>1\*</sup>

*Virology Division, Department of Infectious Diseases and Immunology, Utrecht University, 3584 CL Utrecht, The Netherlands,<sup>1</sup> and Division of Gene Therapy, Department of Medical Oncology, VU University Medical Center, 1081 HV Amsterdam, The Netherlands<sup>2</sup>*

Received 11 August 2005/Accepted 8 November 2005

**Murine hepatitis coronavirus (MHV)-A59 infection depends on the interaction of its spike (S) protein with the cellular receptor mCEACAM1a present on murine cells. Human cells lack this receptor and are therefore not susceptible to MHV. Specific alleviation of the tropism barrier by redirecting MHV to a tumor-specific receptor could lead to a virus with appealing properties for tumor therapy. To demonstrate that MHV can be retargeted to a nonnative receptor on human cells, we produced bispecific adapter proteins composed of the N-terminal D1 domain of mCEACAM1a linked to a short targeting peptide, the six-amino-acid His tag. Preincubation of MHV with the adapter proteins and subsequent inoculation of human cells expressing an artificial His receptor resulted in infection of these otherwise nonsusceptible cells and led to subsequent production of progeny virus. To generate a self-targeted virus able to establish multiround infection of the target cells, we subsequently incorporated the gene encoding the bispecific adapter protein as an additional expression cassette into the MHV genome through targeted RNA recombination. When inoculated onto murine LR7 cells, the resulting recombinant virus indeed expressed the adapter protein. Furthermore, inoculation of human target cells with the virus resulted in a His receptor-specific infection that was multiround. Extensive cell-cell fusion and rapid cell killing of infected target cells was observed. Our results show that MHV can be genetically redirected via adapters composed of the S protein binding part of mCEACAM1a and a targeting peptide recognizing a nonnative receptor expressed on human cells, consequently leading to rapid cell death. The results provide interesting leads for further investigations of the use of coronaviruses as antitumor agents.**

The ability to genetically modify viral genomes has greatly increased the opportunities of developing viruses for tumor therapy. The main aim of designing tumor-selective viruses is to generate agents with destructive potency toward cancer cells but without or with only limited pathogenicity to normal tissues. This goal can be achieved either by engineering viruses with a preference for replication in cancer cells or by constructing viruses with a tumor-selective tropism (reviewed in references 37 and 40). To achieve the latter requires viruses to be redirected to tumor-specific antigens.

Coronaviruses, a family of positive-strand enveloped RNA viruses of the order *Nidovirales*, have several characteristics that make them attractive as oncolytic viruses. First, they have a very narrow host range, determined by the interaction of their spike (S) glycoprotein (a class I fusion protein) and their cellular receptor. For instance, the host cell tropism of murine hepatitis coronavirus (MHV) strain A59 is determined by the specific interaction between its S protein and the murine carcinoembryonic antigen cell adhesion protein 1a (mCEACAM1a) (1, 9, 11, 32, 52, 55). The presence of this receptor on the cell is a major prerequisite for infection, as cells that are normally nonsusceptible can be efficiently infected and killed once made to express the mCEACAM1a molecule (11, 14, 38, 39). Since

mCEACAM1a is not expressed on human cells, MHV-A59 cannot establish an infection of such cells, either normal or cancer cells. Therefore, redirecting the virus to an antigen on human cancer cells is likely to be sufficient for establishing a specific infection of these cells. A second feature making MHV particularly favorable as an oncolytic agent is that infection of susceptible cells gives rise to the formation of large multinucleated syncytia by the recruitment of surrounding uninfected cells (50). This characteristic property, in combination with its short replication cycle (6 to 9 h), makes it possible for MHV to rapidly kill cells once they are infected. We therefore hypothesize that MHV-A59, once redirected to human cancer cells, might be a potential new antitumor virus.

The MHV-A59 spike protein is a type I transmembrane glycoprotein of 180 kDa. It is proteolytically cleaved by furin, resulting in an amino (N)-terminal S1 protein and a membrane-anchored S2 protein. Upon binding of the N-terminal 330 amino acids of S1 (46) to residues in the N-terminal immunoglobulin (Ig)-like domain (D1) of mCEACAM1a (12, 25, 39, 48, 49, 51), a conformational change in the spike protein that leads to the exposure of the fusion peptide and its insertion into the target cell membrane is induced (28, 30, 49, 56). Upon binding of the soluble form of the mCEACAM1a molecule to the spike protein, a similar conformational change in the spike protein is induced (30, 49, 56), with concomitant reduction of virus infectivity. Here we hypothesize that a soluble receptor domain of mCEACAM1a linked to a targeting peptide that can bind to a nonnative receptor can be used to redirect MHV to normally nonsusceptible target cells.

\* Corresponding author. Mailing address: Virology Division, Department of Infectious Diseases and Immunology, Utrecht University, 3584 CL Utrecht, The Netherlands. Phone: 31 30 253 2485. Fax: 31 30 253 6723. E-mail: p.j.m.rottier@vet.uu.nl.

† M.H.V. and T.W. contributed equally to this study.

Recently, we demonstrated that feline infectious peritonitis virus can be redirected to the nonnative epidermal growth factor receptor by applying a bispecific single-chain antibody during inoculation (54). To generate a virus able to produce this device and grow on epidermal growth factor receptor-positive cells independently, we attempted to incorporate the gene encoding the antibody into the feline infectious peritonitis virus genome. This failed, probably because of high instability of the foreign gene in the genome due to its specific nucleotide composition. In the present study, we therefore used a targeting adapter composed of the virus-binding N-terminal domain of the mCEACAM1a MHV receptor (15) fused to a short targeting peptide, the six-amino-acid His tag, to redirect MHV (53). Our results show that the adapter proteins, when produced using a vaccinia virus expression system, were able to target MHV to cells expressing a surface-displayed single-chain variable antibody fragment (sFv) with specificity for a C-terminal His (sFvHis). Subsequent incorporation of the adapter gene as an additional expression cassette in the MHV genome to allow multiround infection indeed resulted in extensive cell-cell fusion and efficient cell killing of the target cells.

#### MATERIALS AND METHODS

**Viruses and cells.** Recombinant felinized MHV (fMHV) (26) stocks were produced and titrated in parallel on *Felis catus* whole fetus (FCWF) cells (obtained from N. C. Pedersen). Mouse LR7 cells (26) were used to analyze and propagate the recombinant MHV-A59-derived viruses.

Murine LR7 cells, feline FCWF-4 cells, murine Ost-7 cells (obtained from B. Moss), human U118MG cells, His receptor-expressing U118MG cells (U118MG-HissFv.rec; kindly provided by J. Douglas [8]), human 293 cells, and His receptor-expressing 293 cells (293-HissFv.rec; kindly provided by J. Douglas [8]) were grown in Dulbecco's modified Eagle's medium (DMEM) (Cambrex Bio Science, Verviers, Belgium) containing 10% fetal calf serum, 100 IU of penicillin/ml, and 100 µg of streptomycin/ml (all from Life Technologies, Ltd., Paisley, United Kingdom). U118MG-HissFv.rec and 293-HissFv.rec culture medium contained 0.25 mg/ml G418 (Life Technologies, Ltd., Paisley, United Kingdom).

**Construction of the genes encoding the adapter proteins soR-His and soR-h-His.** In order to obtain the gene fragment encoding the amino-terminal D1 domain of the mCEACAM1a receptor (this domain is further referred to as soR), PCR was performed with pCEP4:sMHV-R-Ig (kindly provided by Thomas Gallagher [15]), using forward primer 2296 (5'-CATGGGCCAGCCGCGCG AGCTGGCCTCAGCACAT-3', nucleotides [nt] 4 to 22 of mCEACAM1a) and reverse primer 2297 (5'-CATGGCGCGCGCGGGGTGTACATGAAATCG-3', nt 409 to 426 of mCEACAM1a). In addition, three subsequent PCRs were performed with the same plasmid, using primers 2296 and 2298 (5'-TGTCACA AGATTTGGGCTGGGGTGTACATGAAATCG-3', nt 409 to 426 of mCEACAM1a), 2296 and 2299 (5'-CGGTGGGCATGTGTGAGTTTTGTACAAGA TTTG-3'), and 2296 and 2300 (5'-CATGGCGCGCGCTGGGCACGGTGGG CATGTGT-3') to generate a similar soR fragment but carrying a 3' extension encoding a hinge linker region derived from IgG1 (15), as the authentic mCEACAM1a occurs as a dimer (10). The resulting DNA fragments soR (429 nt) and soR-h (472 nt) (where h is the hinge-encoding region) contained a 5' SfiI site and a 3' NotI site (underlined in the primers) and were subsequently cloned using these restriction enzymes into the expression vector pSecTag2 (Invitrogen, Breda, The Netherlands). The resulting expression vectors, pSTsoR-His and pSTsoR-h-His, encode the N-terminal D1 domain of mCEACAM1a in fusion with an amino-terminal Igκ signal sequence and a carboxy-terminal myc tag and His tag under the control of a cytomegalovirus and a T7 promoter. The hinge region in pSTsoR-h-His is located directly downstream of the D1 domain of mCEACAM1a. The composition of the genes encoding the adapter proteins was confirmed by sequencing.

**Production of the adapter proteins soR-His and soR-h-His.** The adapter proteins soR-His and soR-h-His were produced in a way similar to that described previously for bispecific single-chain variable fragments (54). Briefly, vTF7-3 (13)-infected Ost7 cells were transfected with pSTsoR-His and pSTsoR-h-His by use of Lipofectin (Life Technologies, Ltd., Paisley, United Kingdom). The cul-

ture supernatant was harvested at 20 h postinfection (h p.i.), the proteins were separated from vTF7-3 virus by pelleting the latter by centrifugation with a 20% sucrose cushion, and the adapter proteins in the culture supernatant were concentrated with a Vivaspin20 filter column (Vivascience AG, Hannover, Germany). The concentrations of the proteins were determined by dot blot analysis of serial dilutions of the adapter proteins, with reference to a standard curve similarly prepared with purified N-CEACAM-Fc protein (100 nM). Quantifications were done by immunoassay using antibodies directed against N-CEACAM-Fc, performed as described below for Western blotting. The density multiplied by the surface area of each dot was measured using a densitometer (Bio-Rad Laboratories) and plotted against the corresponding dilution factor, after which the adapter protein concentrations were calculated. The different adapter preparations were brought to the same concentration with culture medium before use.

**Western blotting.** Equal volumes of the concentrated culture supernatant, containing the adapter proteins soR-His and soR-h-His, were subjected to 15% sodium dodecyl sulfate-polyacrylamide gel electrophoresis (SDS-PAGE) in the presence or absence of β-mercaptoethanol. The proteins were blotted onto a polyvinylidene difluoride membrane (Bio-Rad Laboratories, Hercules, Calif.), and the blot was further processed using antibodies directed against N-CEACAM-Fc (1:3,000; kindly provided by Thomas Gallagher [15]) and swine anti-rabbit peroxidase (1:3,000; DakoCytomation, Glostrup, Denmark). The proteins were visualized by enhanced chemiluminescence (Amersham Pharmacia Biotech Europe GmbH, Freiburg, Germany).

**Determination of firefly expression.** Monolayers of  $1 \times 10^5$  293-HissFv.rec and U118MG-HissFv.rec cells were inoculated with  $1 \times 10^4$  50% tissue culture infective doses (TCID<sub>50</sub>) (as determined by endpoint dilution on LR7 cells) of the firefly luciferase-expressing MHV-EFLM (4) preincubated at 4°C for 1 h with the indicated amounts of adapter proteins. At the indicated time points, the cells were lysed using the appropriate buffer provided with the firefly luciferase assay system (Promega Corporation, Madison, Wis.). Intracellular luciferase expression was measured according to the manufacturer's instructions, and the relative light units (RLU) were determined with a luminometer (Turner Biosystems, Sunnyvale, Calif.).

**Fluorescence-activated cell sorter (FACS) analysis.** The cell lines 293-HissFv.rec and U118MG-HissFv.rec were analyzed for relative sFvHis receptor expression by exploitation of the presence of an extracellular hemagglutinin (HA) tag C terminal of sFvHis (8). To this end, U118MG, U118MG-HissFv.rec, 293, and 293-HissFv.rec cells were collected, incubated either in the presence or in the absence of anti-HA high-affinity antibody (1:250; Roche Diagnostics GmbH, Mannheim, Germany), and subsequently incubated with goat anti-rat fluorescein isothiocyanate (FITC) (1:200; DakoCytomation, Glostrup, Denmark). Flow cytometry was performed using FACScan analysis (Becton Dickinson, Erembodegem-Aalst, Belgium). The relative geometric mean (GM) fluorescence of each cell line in the presence or absence of anti-HA high-affinity antibody was determined by using WinMDI 2.8 (<http://facs.scripps.edu/>). The GM ratio indicates the sFvHis expression level of an sFvHis-expressing cell line relative to that of the parental cell line.

**Construction of the vectors for targeted recombination.** To allow expression of the adapter proteins from an additional expression cassette in the viral genome of MHV-A59, a transcription regulation sequence (TRS) (underlined in the primers given below) was first introduced into pSTsoR-His and pSTsoR-h-His directly upstream of the soR-encoding region, as described before for pXH1bMS (5). To this end, the plasmids were digested with NheI and subsequently the oligonucleotides 1838 (5'-CTAGCGATATCTAATCTAAACTTTAG-3') and 1839 (5'-CTAGCTAAAGTTTAGATTAGATATCG-3'), containing NheI site extensions, were ligated into this site, resulting in pST-T-soR-His and pST-T-soR-h-His, respectively. The presence and orientation of the TRS were confirmed by sequencing. Next, the fragments TRS-soR-His and TRS-soR-h-His were obtained from pST-T-soR-His and pST-T-soR-h-His, respectively, by digestion of the vectors with EcoRV and PmeI and the purified fragments were cloned into the Klenow-treated HindIII site of pXH1802 (3), containing approximately 1,200 bp of the 3' end of the replicase gene 1b fused to the S gene of MHV-A59. Then, the resulting plasmids were digested with RsrII and AvrII and the obtained fragments were cloned into pMH54 (26), treated with the same enzymes. This resulted in the transcription vectors pMHsoR-His and pMHsoR-h-His, suitable for targeted recombination. The transcription vector in which the RsrII-AvrII fragment from pXH1802 was cloned into the corresponding sites of pMH54 was used as a control vector for targeted recombination (further referred to as pXHd2aHE [3]).

**Targeted recombination.** The adapter genes soR-His and soR-h-His were introduced as additional expression cassettes into the MHV genome by targeted RNA recombination as described previously (3, 26). Briefly, donor RNAs tran-

scribed *in vitro* from PacI-linearized plasmids pXHd2aHE, pMHsoR-His, and pMHsoR-h-His were transfected by electroporation into feline FCWF-4 cells that had been infected with fMHV at a multiplicity of infection (MOI) of 0.5 4 h earlier. These cells were then plated in culture flasks, and the culture supernatant was harvested 24 h later. Progeny virus was plaque purified, and virus stocks were grown on LR7 cells. After confirmation of the presence of the additional expression cassettes by reverse transcription-PCR (RT-PCR) with purified viral RNA from these virus stocks, the virus titers of the stocks were determined by endpoint dilution on LR7 cells. These passage 2 virus stocks were subsequently used in the experiments. For each virus, two independent recombinants were generated as a control for effects caused by unintended mutations in other parts of the viral genome.

**Viral RNA isolation and RT-PCR.** First, from 140  $\mu$ l virus-containing culture supernatant, viral RNA was isolated using a QIAGEN viral RNA isolation kit (according to the manufacturer). Reverse transcription with the isolated RNA was then performed using reverse primer 1127 (5'-CCAGTAAGCAATAATG TGG-3'), located at nt 24,110 to 24,128 of the MHV genome (GenBank accession no. NC 001846). PCR was performed using primers 1173 (5'-GACTTAG TCCTCTCCTTGATTG-3', nt 21650 to 21671) and 1260 (5'-CTTCAACGGTC TCAGTGC-3', nt 24,041 to 24,058), overlapping the region that contains the inserted expression cassette. The resulting fragments were subsequently sequenced to confirm the sequence of the inserts.

**Analysis of viral growth kinetics.** An amount of  $1 \times 10^5$  cells per 2-cm<sup>2</sup> well of the indicated cells was inoculated with  $0.5 \times 10^5$  TCID<sub>50</sub> (as determined by endpoint dilution on LR7 cells). After 1 h, the culture supernatant was removed, the cells were washed, and fresh culture medium was added. At several time points *p.i.*, the medium was harvested and stored at -80°C until analysis. The amount of virus produced at each time point was determined by endpoint dilution on LR7 cells, and TCID<sub>50</sub> values were calculated.

**Immunofluorescence assay.** For indirect immunofluorescence, LR7 cells were grown on 10-mm coverslips and infected with the recombinant MHV viruses at an MOI of 0.5. The cells were fixed at 5 h *p.i.*, permeabilized, and processed for double labeling. Incubations were subsequently performed with rabbit polyclonal MHV antiserum K134 (1:400) (41), goat anti-rabbit FITC (1:200; ICN-Cappel, Aurora, Ohio), monoclonal antibody directed against the C-terminal His<sub>6</sub> tag (1:100; Invitrogen, Woerden, The Netherlands), and donkey anti-mouse Cy5 (1:100; Jackson ImmunoResearch, West Grove, Pa.). The staining was visualized using a Leica TCS SP confocal laser scanning microscope and Leica software ([http://www.confocal-microscopy.com/website/sc\\_llt.nsf](http://www.confocal-microscopy.com/website/sc_llt.nsf)).

**Immunoperoxidase staining of cells.** An amount of  $1 \times 10^5$  293-HissFv.rec and U118MG-HissFv.rec cells was inoculated with  $0.5 \times 10^5$  TCID<sub>50</sub>. At 16 h *p.i.*, the cells were fixed and stained to analyze expression of viral proteins. The cells were incubated with rabbit polyclonal MHV antiserum K134 (1:300) (41), followed by incubation with swine anti-rabbit peroxidase (1:300; DakoCytomation, Glostrup, Denmark) and staining using 3-amino-9-ethylcarbazole (Brunschwig, Amsterdam, The Netherlands) according to the manufacturer's protocol.

**Metabolic labeling and radioimmunoprecipitation.** Subconfluent monolayers of LR7 cells were infected with the recombinant viruses at an MOI of 1. At 5.5 h *p.i.*, the cells were washed and starved for 30 min in cysteine- and methionine-free DMEM containing 5% fetal calf serum, 1 mM Glutamax, and 10 mM HEPES, pH 7.3 (all from Life Technologies, Ltd., Paisley, United Kingdom). The cells were labeled for 1 h with <sup>35</sup>S-Translabel (Amersham Pharmacia Biotech Europe GmbH, Germany) and chased with nonradioactive culture medium for 3 h. Culture supernatants were used for immunoprecipitation using antibodies directed against N-CEACAM-Fc.

**Monolayer cytotoxicity analysis.** An amount of  $5 \times 10^4$  293-HissFv.rec cells per 0.32-cm<sup>2</sup> well was seeded and infected in triplicate with various amounts of MHVsoR-h-His. At several time points after inoculation, the culture medium was replaced by DMEM containing 10% WST-1 (Roche Diagnostics GmbH, Mannheim, Germany) and the cells were cultured for 2 h. Thereafter, the optical density at 450 nm was measured and the viability of the infected cells was calculated relative to that of uninfected control cells after subtraction of background values of WST-1 incubated in the absence of cells.

## RESULTS

**Generation of soR-His and soR-h-His adapter proteins.** To explore the possibilities of redirecting MHV to a nonnative receptor on human cells (Fig. 1A), we generated adapter proteins composed of the N-terminal D1 domain of the MHV receptor mCEACAM1a linked via a stretch of three alanine

residues and a myc tag to a six-amino-acid His tag. The genes encoding these adapter proteins were preceded by a sequence encoding the Ig $\kappa$  signal peptide and constructed either without or with a hinge-encoding region (h) of an IgG molecule directly downstream of the soR, resulting in soR-His and soR-h-His, respectively (Fig. 1B). The Ig $\kappa$  signal sequence would direct adapter protein secretion, the soR would provide for binding to and induction of a conformational change in the spike protein, and the His tag would effect the binding to a nonnative sFvHis receptor on target cells. Furthermore, the hinge region would allow dimerization of the adapter protein soR-h-His, as occurs with the natural mCEACAM1a receptor (10, 15), whereas the adapter protein soR-His would remain in a monomeric state.

Both adapter proteins were expressed using a vaccinia virus T7 expression system in Ost-7 cells. Western blot analysis (Fig. 1C) of the culture supernatants electrophoresed under reducing conditions using antibodies directed against N-CEACAM-Fc (15) showed that the adapter proteins soR-h-His and soR-His were produced (Fig. 1C, left), whereas no protein was detected in culture supernatant from mock-transfected cells. The apparent sizes of soR-His and soR-h-His proteins were somewhat larger than their predicted sizes of 18.4 and 20.0 kDa, respectively. Treatment of the resulting proteins with endoglycosidase H reduced their apparent sizes, confirming that both soR-His and soR-h-His were N glycosylated (data not shown). Analysis of the adapter proteins under nonreducing conditions (Fig. 1C, right) demonstrated that soR-h-His migrated at 55 to 60 kDa, which is consistent with the size of an soR-h-His dimer. Hence, the presence of a hinge region in the protein indeed induced dimerization of soR-h-His. In contrast, the size of the soR-His protein analyzed under nonreducing conditions was similar to that analyzed under reducing conditions, indicating that it was produced as a monomer.

**The adapter proteins soR-His and soR-h-His can redirect MHV to the nonnative sFvHis receptor on human cells.** To study the ability of the adapter proteins to redirect MHV to the corresponding nonnative receptor, we selected two human cell lines, 293-HissFv.rec and U118MG-HissFv.rec (8), that express a surface-displayed single-chain variable fragment (sFv) with specificity for a C-terminal His tag (sFvHis) (27). FACS analysis (Fig. 2A) was performed to determine relative sFvHis expression for these cells. GM ratios of 16.5 (293-HissFv.rec cells) (Fig. 2A, left) and 1.8 (U118MG-HissFv.rec cells) (Fig. 2A, right) were observed. This confirmed that both cell lines expressed sFvHis but indicated that the expression level was much higher with the 293-HissFv.rec cells than with the U118MG-HissFv.rec cells.

Next, we analyzed whether soR-His and soR-h-His were able to redirect MHV-EFLM, an MHV-A59 derivative expressing firefly luciferase (4), to sFvHis on 293-HissFv.rec and U118MG-HissFv.rec cells. To this end,  $1 \times 10^4$  TCID<sub>50</sub> of MHV-EFLM (as determined by endpoint dilution on LR7 cells) were incubated with the indicated amounts of soR-His or soR-h-His (Fig. 2B) and subsequently inoculated onto  $1 \times 10^5$  293-HissFv.rec or U118MG-HissFv.rec cells. Luciferase activity was measured to determine whether inoculation had resulted in successful infection of the target cells. The data show that both soR-His and soR-h-His were able to redirect MHV-EFLM to 293-HissFv.rec and U118MG-HissFv.rec cells,

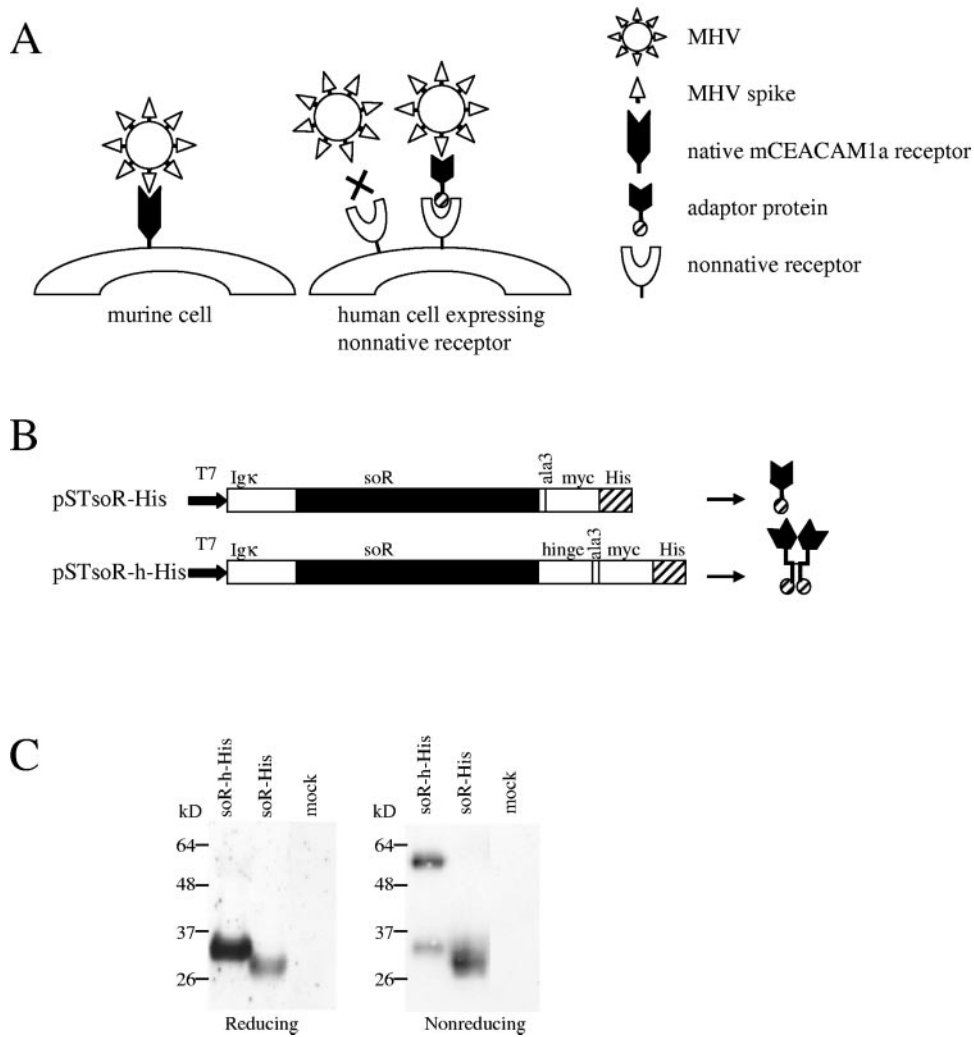


FIG. 1. Approach to redirect MHV to a nonnative receptor. (A) Rationale for using adapter proteins to redirect MHV to a nonnative receptor present on human cells. (B) Schematic diagram of the expression cassettes of pSTsoR-His and pSTsoR-h-His and the designs of the adapter proteins soR-His and soR-h-His. The Igk signal sequence directs adapter protein secretion, the N-terminal D1 domain of mCEACAM1a (soR) provides for binding to and induction of conformational changes in the MHV spike protein, and the six-amino-acid His tag (His) provides for binding to the artificial sFvHis receptor. The hinge (h) linker region present in soR-h-His should allow formation of disulfide-linked dimers of the resulting protein (T7, T7 promoter; myc, myc tag; ala3, three alanine residues). The resulting adapter proteins are depicted on the right. (C) Western blot analysis of soR-h-His and soR-His adapter proteins. Ost-7 cells were infected with vaccinia vTF7-3 and transfected with the plasmids pSTsoR-h-His and pSTsoR-His. Mock transfection was done as a control. The culture supernatants were analyzed by Western blotting using antibodies directed against N-CEACAM-Fc (15) under both reducing and nonreducing conditions. In each case, the positions of marker proteins run in the same gel are shown at the left.

whereas target cells inoculated with mock-preincubated MHV-EFLM remained uninfected, indicating that the infection was mediated specifically by the adapter proteins. This was confirmed by similar inoculations of the parental cell lines 293 and U118MG, which resulted in only background levels of luciferase activity (data not shown).

Consistently, the infection efficiencies were clearly dependent on the amount of adapter protein present. In both cell lines, luciferase expression increased upon inoculation of similar amounts of MHV-EFLM in the presence of increasing amounts of soR-His and soR-h-His (Fig. 2B). Strikingly, luciferase expression was consistently much higher for soR-h-His-mediated infection than with soR-His, as can be observed by

comparing the potencies of similar amounts of adapter proteins. In addition, luciferase activity was invariably higher when targeting MHV-EFLM to 293-HissFv.rec cells than to U118MG-HissFv.rec cells. This can be explained, at least in part, by the different levels of sFvHis receptor expressed with these cells. However, we cannot exclude that MHV replication and thus protein expression in U118MG-HissFv.rec cells were inherently lower than in 293-HissFv.rec cells.

**Targeted MHV infection requires the native spike membrane fusion function.** To investigate whether the adapter-mediated entry of MHV into human cells occurs by the same membrane fusion mechanism used by the virus to naturally infect murine cells, we applied an inhibitor known to specifi-

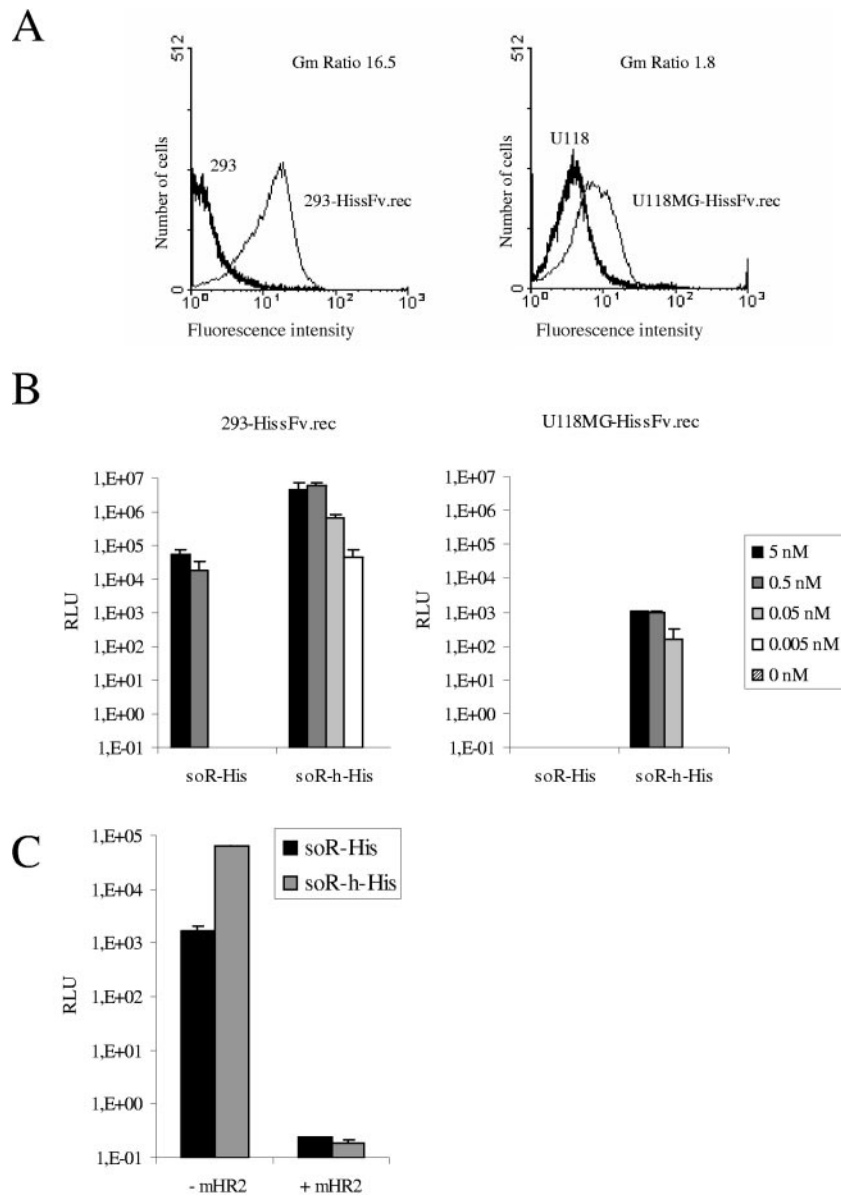


FIG. 2. Redirection of MHV to an artificial sFvHis receptor expressed on human cells by using the adapter proteins soR-His and soR-h-His. (A) FACS analysis of the target cell lines 293-HissFv.rec and U118MG-HissFv.rec and their parental cell lines, 293 and U118MG. Flow cytometry was performed using the anti-HA high-affinity antibody to determine the expression of sFvHis for each cell line. The indicated GM ratios relate to the ratio of relative GM fluorescence between 293-HissFv.rec and 293 cells (left) and between U118MG-HissFv.rec and U118MG cells (right) and are an indication of the relative amounts of sFvHis expression for the target cell lines. (B) Inoculation of human sFvHis-expressing cells with MHV-EFLM in the presence or absence of the adapter proteins soR-His and soR-h-His. Monolayers of  $1 \times 10^5$  293-HissFv.rec and U118MG-HissFv.rec cells were inoculated with firefly luciferase-expressing MHV virus MHV-EFLM (4) preincubated with the indicated amounts of soR-His, soR-h-His, or mock culture supernatant, as described in Materials and Methods. The cells were lysed 20 h p.i., and luciferase activity (in RLU) was measured using a luminometer. (C) Redirection of MHV-EFLM using soR-His and soR-h-His proteins can be blocked with the MHV-specific fusion inhibitor mHR2 (2). 293-HissFv.rec cells were inoculated with MHV-EFLM preincubated with 0.5 nM soR-His or soR-h-His in the absence (– mHR2) or presence (+ mHR2) of 20  $\mu$ M mHR2 peptide. Intracellular luciferase activity (in RLU) was determined at 18 h p.i. For panels B and C, the values depicted are the means of an experiment performed in triplicate; bars show standard deviations.

cally block this process. 293-HissFv.rec cells were inoculated with MHV-EFLM preincubated with 0.5 nM soR-His or soR-h-His in the presence or absence of 20  $\mu$ M of mHR2, a peptide fusion inhibitor derived from the C-terminal heptad repeat region (HR2) of the MHV S protein (2). As is clear from Fig. 2C, luciferase expression was efficiently blocked by the peptide,

indicating that adapter-targeted MHV infection is dependent on S-mediated membrane fusion.

**Generation and growth characteristics of recombinant MHVsoR-His and MHVsoR-h-His viruses.** Having demonstrated that MHV can be retargeted by an exogenously added adapter protein, our next aim was to incorporate this informa-

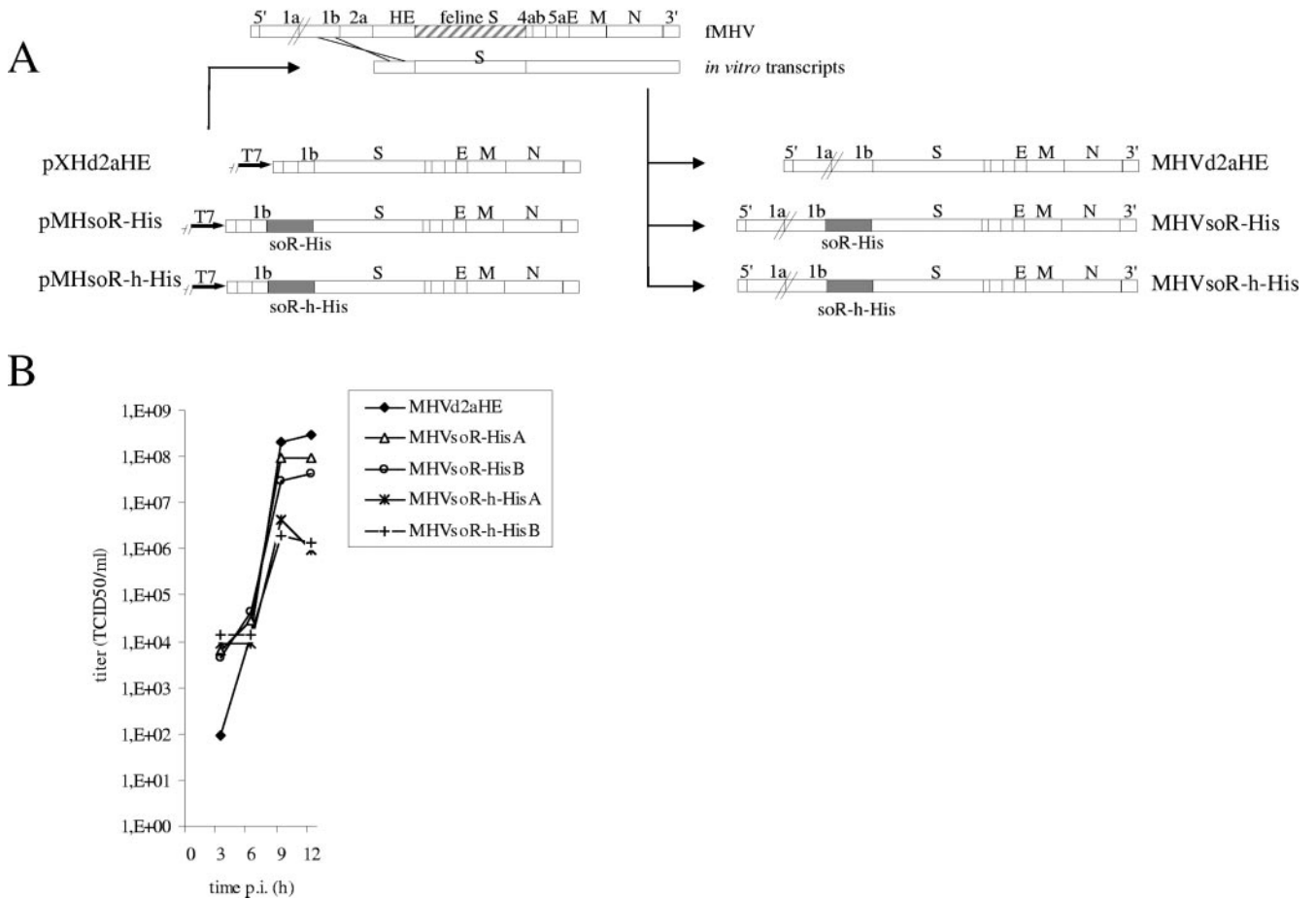


FIG. 3. Recombinant MHVsoR-His and MHVsoR-h-His viruses and their growth kinetics with murine cells. (A) Targeted recombination vectors, recombination procedure, and resulting viral genomes. The transcription vectors from which the RNAs were transcribed *in vitro* by T7 RNA replicase are depicted on the left side. The inserted additional expression cassettes encoding soR-His and soR-h-His are represented by gray boxes. The recombinant viruses generated by targeted recombination are depicted at the right. (B) Single-step growth kinetics of the MHV recombinants in LR7 cells. LR7 cells were infected with the MHV recombinants at an MOI of 0.5, production of progeny virus in the culture supernatant at different times p.i. was determined by endpoint dilution on LR7 cells, and TCID<sub>50</sub> values were calculated. Viruses marked A and B represent independently generated recombinants. In each case, the growth curve shown is a representative example of two independent experiments.

tion into the viral genome to generate a virus producing its own targeting device, thereby acquiring the ability to be independently propagated on the target cells. To this end, the soR-His and soR-h-His expression cassettes were provided with a TRS to allow transcription of the foreign gene from the viral genome (4) and inserted into the recombination vector pMH54, thereby replacing the genes 2a and HE from MHV-A59 (Fig. 3A). To obtain the recombinant MHV viruses, targeted recombination was performed as described earlier (26), resulting in the viruses MHVsoR-His and MHVsoR-h-His (Fig. 3A). In parallel, a control recombinant MHV that lacks the genes 2a and HE was generated, resulting in MHVd2aHE. The genotypes of the recombinant passage 2 viruses were confirmed by RT-PCR with viral RNA isolated after plaque purification and stock production with murine LR7 cells (data not shown).

The *in vitro* growth kinetics of the recombinant MHVsoR-His and MHVsoR-h-His viruses were compared with that of MHVd2aHE by comparing their one-step growth curves with murine LR7 cells (Fig. 3B). Pairs of independently generated

recombinant viruses were used to verify that the observed phenotypes were not a consequence of unintended mutations. The recombinant MHVsoR-His viruses appeared to replicate very similarly to MHVd2aHE, whereas MHVsoR-h-His viruses grew with similar kinetics but to considerably lower titers. The yields of MHVsoR-h-His were almost 2 log units lower than those of MHVsoR-His and MHVd2aHE.

**MHV recombinant viruses are able to express and secrete the adapter proteins from infected murine LR7 cells.** To demonstrate that the adapter proteins soR-His and soR-h-His were produced from their respective expression cassettes in the recombinant MHVsoR-His and MHVsoR-h-His viruses, murine LR7 cells were inoculated with the recombinant MHV viruses and processed for a double immunofluorescence labeling. The following antibodies were used in successive order: anti-MHV serum, FITC-labeled secondary antibody, anti-His<sub>6</sub> (C-terminal) monoclonal antibody, and Cy-5 secondary antibody. Confocal scanning laser microscopy performed with the processed cells showed His staining in cells infected with either virus (Fig.

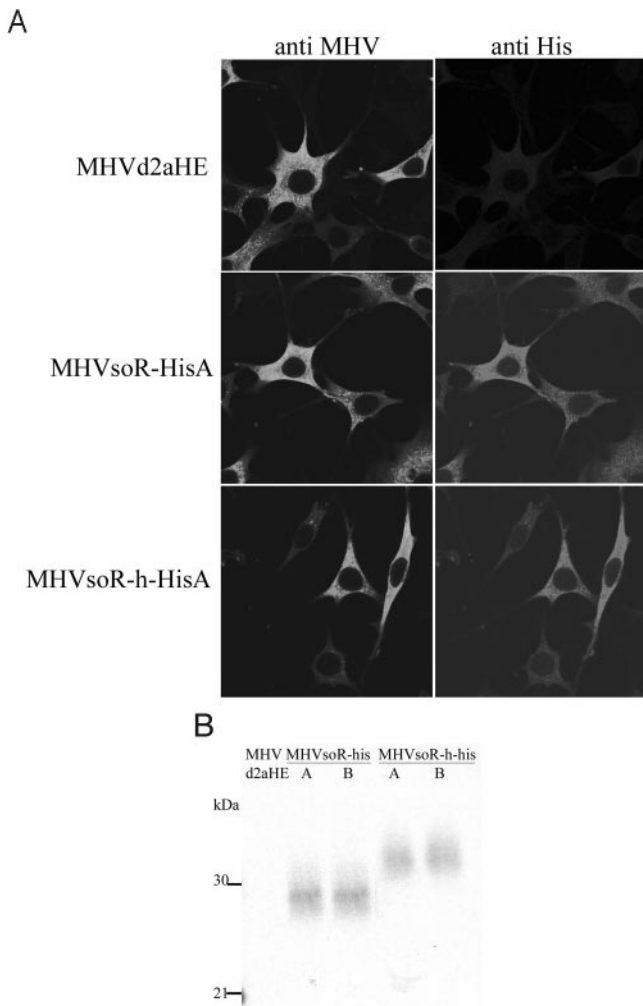


FIG. 4. Expression of soR-His and soR-h-His by MHV recombinant viruses. (A) Confocal laser scanning microscopy of LR7 cells infected with MHVd2aHE, MHVsoR-His, and MHVsoR-h-His recombinant viruses. LR7 cells were infected with recombinant viruses at an MOI of 0.5, fixed at 6 h p.i., permeabilized, and processed for immunofluorescence by subsequently applying the anti-MHV serum K134, a green fluorescent FITC secondary antibody, the anti-His<sub>6</sub> (C-terminal) antibody, and a red fluorescent Cy5 secondary antibody ( $\times 100$  magnification). The staining was visualized using a Leica TCS SP confocal laser scanning microscope by excitation at 488 nm (FITC; left column) or 568 nm (Cy5; right column). For each recombinant MHV virus, one representative example of the independently generated viruses is shown. (B) Radioimmunoprecipitation of the secreted soR-His and soR-h-His proteins. LR7 cells were inoculated with MHVd2aHE, MHVsoR-His, and MHVsoR-h-His at an MOI of 1 and subsequently labeled with  $^{35}\text{S}$ -labeled Met/Cys from 6 to 7 h p.i. and chased with cold medium for 3 h. Immunoprecipitation was performed with the culture medium by use of anti-N-CEACAM-Fc antibodies (15), and the precipitates were analyzed by SDS-PAGE under reducing conditions. Viruses marked A and B represent independently generated recombinants. The positions of molecular mass marker proteins are indicated to the left of the gel.

4A, middle and bottom) but not in uninfected cells (not shown) or cells infected with the control virus MHVd2aHE-infected LR7 cells (top).

To investigate the excretion of the adapter proteins from

MHVsoR-His- and MHVsoR-h-His-infected cells into the culture supernatant, LR7 cells were infected with the different recombinant viruses at an MOI of 1 and labeled for 3 h with  $^{35}\text{S}$ -labeled amino acids starting at 6 h p.i. Subsequently, the culture supernatants were processed for immunoprecipitation with anti-N-CEACAM-Fc antibodies (15) and analyzed by SDS-PAGE under reducing conditions (Fig. 4B). Diffuse bands representing the proteins soR-His and soR-h-His were observed. The presence of the hinge region in soR-h-His accounts for the difference in size between the two proteins. Their electrophoretic mobilities are similar to those of the proteins expressed from pSTsoR-His and pSTsoR-h-His (Fig. 1C). Analysis of the immunoprecipitates under nonreducing conditions showed that only a small fraction of the soR-h-His adapter protein occurred as dimers (data not shown). In conclusion, MHVsoR-His and MHVsoR-h-His recombinant viruses expressed and excreted the adapter proteins from infected LR7 cells.

**MHVsoR-h-His, but not MHVsoR-His, infects sFvHis-expressing human target cells.** To determine whether the adapter protein-expressing recombinant MHV viruses were able to infect human cells displaying the nonnative sFvHis receptor, 293-HissFv.rec and U118MG-HissFv.rec cells ( $1 \times 10^5$  each) were inoculated with  $0.5 \times 10^5$  TCID<sub>50</sub> of virus grown in and titrated on LR7 cells. The cells were fixed 16 h after inoculation, permeabilized, and stained using polyclonal MHV antiserum (Fig. 5). For both 293-HissFv.rec and U118MG-HissFv.rec cells, positive staining was observed only after inoculation with MHVsoR-h-His recombinant viruses, not after inoculation with MHVsoR-His recombinant viruses. Neither of the two cell lines could be infected with MHVd2aHE, indicating that infection was critically dependent on expressed soR-h-His. Moreover, many more cells became infected after inoculation of 293-HissFv.rec cells than after inoculation of U118MG-HissFv.rec cells. These results are in agreement with the differences in targeting efficiency observed when redirecting MHV-EFLM by means of exogenous soR-h-His protein to these cells (Fig. 2B). Subsequent cell-cell fusion was observed only with 293-HissFv.rec cells and was very obvious 24 h p.i. (Fig. 5, top two panels).

To confirm the specificity of the targeted infection, similar infectious amounts of MHVsoR-h-His viruses were used to inoculate the parental cell lines 293 and U118MG, which lack sFvHis receptor expression. No infected cells could be detected by immunoperoxidase staining, indicating that the infection by MHVsoR-h-His was sFvHis specific (data not shown).

**Analysis of the growth kinetics of and cell killing by the MHVsoR-h-His recombinant viruses in human target cells.** In order to establish whether infection of susceptible cells by MHVsoR-h-His was productive and to determine the kinetics of progeny virus release, we prepared an in vitro growth curve of the virus in 293-HissFv.rec cells. An amount of  $1 \times 10^5$  293-HissFv.rec cells was inoculated with  $0.5 \times 10^5$  TCID<sub>50</sub> of MHVsoR-h-His virus grown in and titrated on LR7 cells. At several time points, samples were taken from the culture supernatant and the infectivity was determined by endpoint dilution on LR7 cells. MHVd2aHE was used as a negative control. Figure 6A shows the results of a representative experiment demonstrating that recombinant MHVsoR-h-His

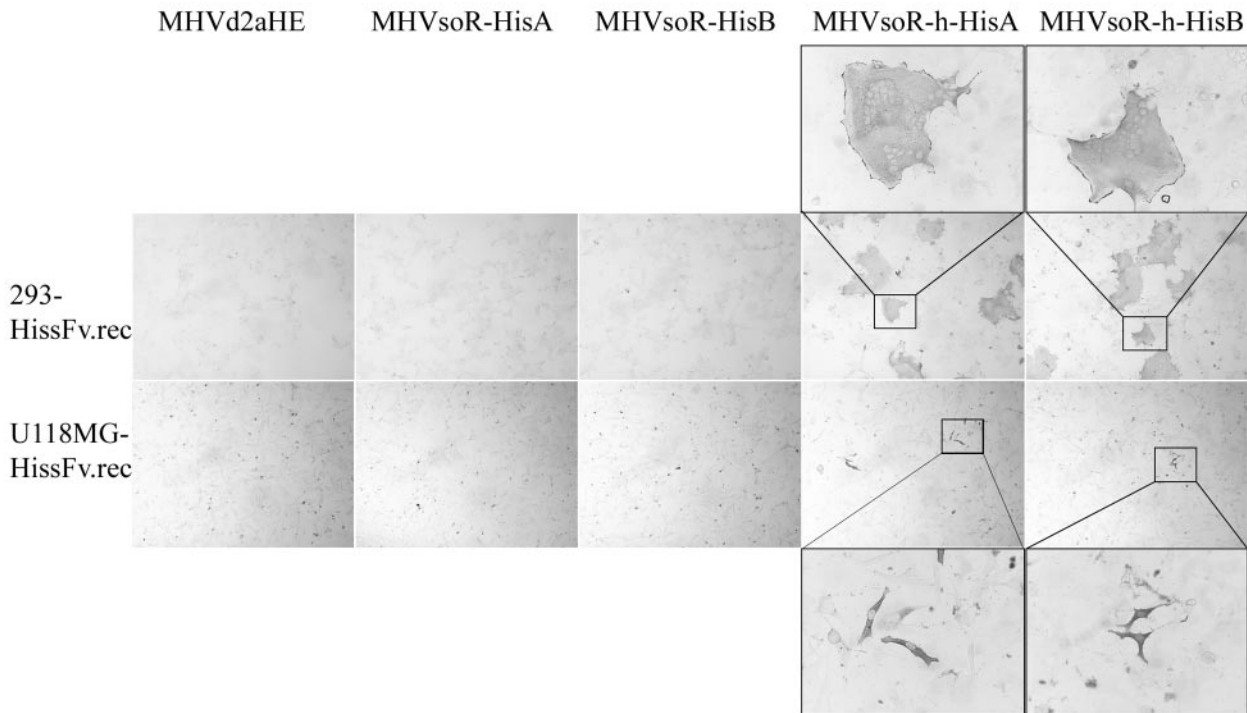


FIG. 5. Immunoperoxidase staining of sFvHis-expressing human cells inoculated with MHVsoR-His and MHVsoR-h-His recombinant viruses. 293-HissFv.rec and U118MG-HissFv.rec cells were inoculated with MHVd2aHE, MHVsoR-His, and MHVsoR-h-His, as described in Materials and Methods. Cells were fixed 16 h after inoculation, permeabilized, and subsequently processed using anti-MHV serum K134. The infection of the target cells was analyzed by 3-amino-9-ethylcarbazole staining. Enlargements of pictures taken at a  $\times 4$  magnification (without a dark border) are shown at a  $\times 10$  magnification (with a dark border). In the enlargements, syncytium formation is clear in 293-HissFv.rec cells infected with MHVsoR-h-His but absent in similarly infected U118MG-HissFv.rec cells.

viruses replicate with normal kinetics and with reasonable yields, with maximal virus titers of  $10^6$  to  $10^7$  TCID<sub>50</sub>/ml as determined by endpoint dilution on LR7 cells.

To confirm that MHVsoR-h-His virus could indeed establish a multiround infection of the target cells, we first produced an MHVsoR-h-His virus stock with 293-HissFv.rec cells and determined the viral titer for murine LR7 cells. Of this virus stock,  $5 \times 10^4$  (1:1) or  $5 \times 10^3$  (1:10) TCID<sub>50</sub> were inoculated onto  $5 \times 10^4$  fresh 293-HissFv.rec cells. Cell viability was measured by WST-1 assay at different time points after inoculation (Fig. 6B). The results indicate that the infection spreads through the 293-HissFv.rec cell culture, killing increasing numbers of cells and eventually eradicating the entire culture. The spread of the infection was confirmed by immunoperoxidase staining of the infected cells at different times p.i., by which an increasing amount of positive cells was observed over time (data not shown). The amount of virus used to inoculate 293-HissFv.rec cells determined the rate at which cell killing occurred; when inoculated at an MOI of 1, destruction of the cell culture took about 24 h, whereas after inoculation at an MOI of 0.1 the process was slower, being essentially complete after about 48 h.

**DISCUSSION**

The results described in this paper demonstrate the feasibility of redirecting recombinant murine coronavirus MHV to a

nonnative receptor on human cells. To achieve this, we introduced bidirectional adapter protein-encoding genes, composed of the spike-binding domain of mCEACAM1a fused to a His tag targeting peptide into the MHV genome. This yielded a recombinant MHV that could establish a receptor-specific infection of sFvHis receptor-expressing human cells, resulting in extensive cell-cell fusion and efficient killing of the target cells.

Many viruses have been explored in various ways for their potential use as oncolytic agents. Several strategies successfully applied genetic modification of viruses to alter their receptor binding specificity and direct them to tumor cells. In some cases, targeting molecules were directly incorporated into the viral surface proteins (7, 17–19, 21, 23, 24, 29, 33, 36, 43–45). Similar strategies were not effective for MHV and fMHV, as viable spike-modified viruses could not be rescued (our unpublished data). This is most probably due to the complex nature and dual function of the S protein, changes in which may easily lead to impairment of the conformational rearrangements in the spike essential for its functioning during cell entry. Soluble receptor proteins have been used to redirect replication-deficient adenoviruses (6, 22) and, very recently, herpes simplex virus (31) to cancer cells. Strikingly, replication-competent adenoviruses were impaired in their oncolytic potential when expressing a soluble receptor targeting molecule (20). Here we have demonstrated that the species barrier of coronaviruses can be alleviated, as shown by the insertion of adapter proteins into the MHV viral genome.

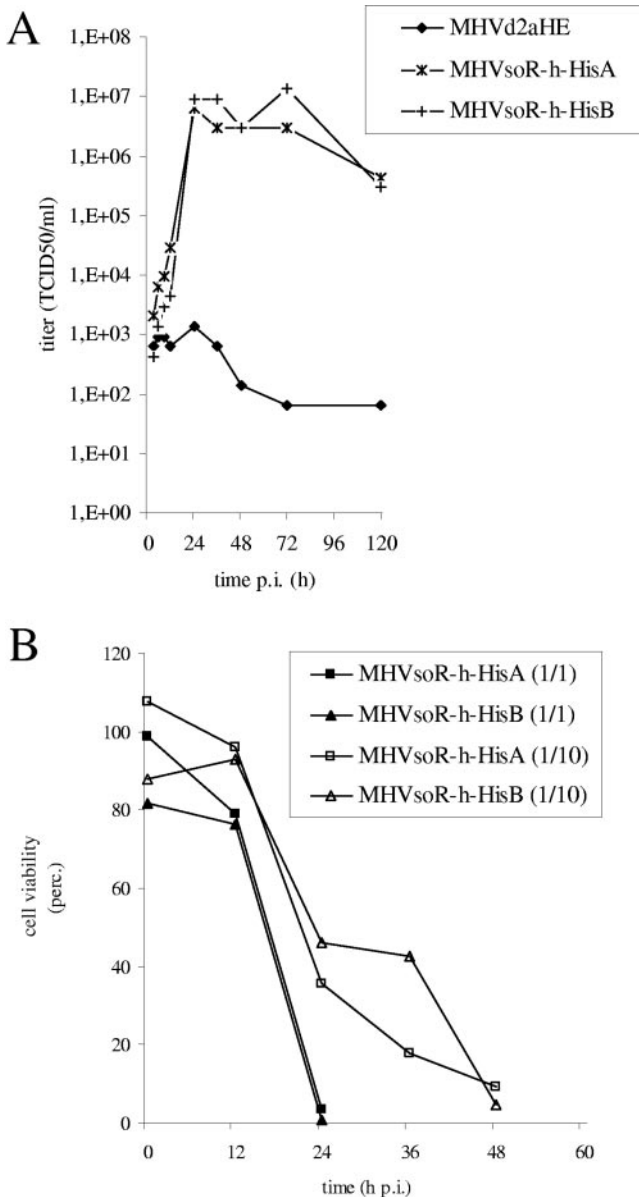


FIG. 6. MHVsoR-h-His progeny virus production and cell killing of 293-HissFv.rec target cells. (A) Growth kinetics of MHVsoR-h-His with 293-HissFv.rec cells. 293-HissFv.rec cells were inoculated with MHVsoR-h-His as described in Materials and Methods. The appearance of progeny virus in the culture media at different times p.i. was determined by endpoint dilution on murine LR7 cells, and TCID<sub>50</sub> values were calculated. (B) Cell viability of 293-HissFv.rec cells after inoculation with MHVsoR-h-His. MHVsoR-h-His virus stocks grown on 293-HissFv.rec cells were used to inoculate fresh 293-HissFv.rec cells. After inoculation of  $5 \times 10^4$  target cells with  $5 \times 10^4$  (1/1) and  $5 \times 10^3$  (1/10) TCID<sub>50</sub> (as determined by endpoint dilution on LR7 cells), cell viability was measured at different time points after inoculation. The indicated optical density at 450 nm values represent the WST-1 values relative to that of uninfected control cells after subtraction of background values of WST-1 incubated in the absence of cells and are the results of an experiment performed in triplicate. perc., percent. The viruses marked A and B indicate the independently generated recombinants.

In general, soluble receptors, i.e., the functional fragments from otherwise membrane-anchored cell surface antigens acting as receptors, bind to viruses and neutralize virus infectivity. These features have been explored in quite some detail for murine coronaviruses (16, 30, 34, 35, 42, 47, 56–58). It has been shown that the N-terminal domain of the mCEACAM1a receptor is sufficient for MHV-A59 binding and for induction of a conformational change in the S protein. This N-terminal domain can block virus infectivity for susceptible cells. Its expression on nonsusceptible cells is only sufficient to render cells susceptible to MHV once a second domain of the mCEACAM1a is also introduced (12) or when it interacts with another unidentified molecule on the plasma membrane (10). Here we demonstrated that when the N-terminal domain of mCEACAM1a is linked to a suitable peptide ligand, the fusion protein can function as an adapter protein that targets MHV to a corresponding receptor on a nonsusceptible cell. The subsequent establishment of infection functionally demonstrates that the adapter protein is sufficient to bind to and induce the conformational changes in the spike essential for MHV infection (15, 48, 56–58).

The efficiency of MHV targeting to a nonnative receptor was critically dependent on the presence of a hinge region in the adapter protein. Adapter proteins containing such a region established a more effective infection of sFvHis-expressing target cells than similar adapter proteins lacking this region. The hinge region might function as an extended linker between the spike-binding domain soR and the target cell receptor, thereby affecting the conformation of the adapter protein or the spacing between the virus membrane and the cell membrane. That the distance between these membranes may be important was also suggested by the results of Dveksler et al. (12), who found that, in contrast to expression of only the N-terminal domain of mCEACAM1a, extension of this domain with a second immunoglobulin-like motif rendered cells susceptible to MHV infection. Alternatively, the formation of disulfide-linked adapter protein dimers might account for the difference in targeting efficiency. Indeed, reduction of the dimer into a monomeric adapter protein by using dithiothreitol led to a drastic decrease in infected target cells (data not shown). Further research is needed to conclusively determine the role of the hinge region in the adapter protein.

The presence of the hinge region also had a pronounced effect on the yields of adapter protein-expressing recombinant MHV viruses from murine LR7 cells. While MHVsoR-His replicated to titers similar to that of the control virus MHVd2aHE, a severe reduction in yield was observed for MHVsoR-h-His (Fig. 3B). It is unlikely that the gene of soR-h-His, larger by merely 51 nucleotides, caused this difference. Since the amounts of the adapter proteins produced by the MHV recombinant viruses were approximately similar (Fig. 4B), it is more likely that the effect is the result of interactions between the adapter proteins and the spike proteins within the infected cell, which might lead to an impairment of virus release. Accordingly, we observed that soR-h-His neutralized MHV infection with murine LR7 cells more efficiently than did soR-His (53). Apparently, the disulfide-linked dimer of soR has a higher affinity for the spike protein than the monomeric form and it thereby acts as a stronger competitor for binding of MHV to cellular mCEACAM1a. The subsequent reduction in

entry of MHVsoR-h-His would explain the lower yield of this virus from mCEACAM1a-expressing cells.

The efficiencies with which our self-targeted MHVs could infect human target cells differed between the two HissFv-expressing cell lines: 293-HissFv.rec cells were the most susceptible, giving rise to extensive cell-cell fusion and ultimately eradication of cell cultures, which was not observed with U118MG-HissFv.rec cells. The significantly higher sFvHis receptor expression with 293-HissFv.rec cells probably accounts for this difference. As a high level of mCEACAM1a expression is also essential for an effective native infection of MHV (9, 11, 38), a similar receptor concentration-dependent infection might apply to nonnative receptors as well. We cannot, however, exclude that other inherent differences between 293-HissFv.rec and U118MG-HissFv.rec cells are responsible for the observed different outcomes.

#### ACKNOWLEDGMENTS

We thank Thomas Gallagher, Joanne Douglas, and Berend-Jan Bosch for providing the pCEP4:SMHVR-Ig plasmid and the antiserum directed against N-CEACAM, for the U118MG-HissFv.rec and 293-HissFv.rec cells, and for the mHR2 fusion inhibitor, respectively.

This work was supported by the Dutch Cancer Society, project UU 2001-2430. V. W. van Beusechem is supported by a research fellowship of the Royal Netherlands Academy of Arts and Sciences (KNAW).

#### REFERENCES

- Beauchemin, N., P. Draber, G. Dveksler, P. Gold, S. Gray-Owen, F. Grunert, S. Hammarstrom, K. V. Holmes, A. Karlsson, M. Kuroki, S. H. Lin, L. Lucka, S. M. Najjar, M. Neumaier, B. Obrink, J. E. Shively, K. M. Skubitz, C. P. Stanners, P. Thomas, J. A. Thompson, M. Virji, S. von Kleist, C. Wagener, S. Watt, and W. Zimmermann. 1999. Redefined nomenclature for members of the carcinoembryonic antigen family. *Exp. Cell Res.* **252**:243–249.
- Bosch, B. J., R. van der Zee, C. A. de Haan, and P. J. Rottier. 2003. The coronavirus spike protein is a class I virus fusion protein: structural and functional characterization of the fusion core complex. *J. Virol.* **77**:8801–8811.
- de Haan, C. A., P. S. Masters, X. Shen, S. Weiss, and P. J. Rottier. 2002. The group-specific murine coronavirus genes are not essential, but their deletion, by reverse genetics, is attenuating in the natural host. *Virology* **296**:177–189.
- de Haan, C. A., L. van Genne, J. N. Stoop, H. Volders, and P. J. Rottier. 2003. Coronaviruses as vectors: position dependence of foreign gene expression. *J. Virol.* **77**:11312–11323.
- de Haan, C. A., H. Volders, C. A. Koetzner, P. S. Masters, and P. J. Rottier. 2002. Coronaviruses maintain viability despite dramatic rearrangements of the strictly conserved genome organization. *J. Virol.* **76**:12491–12502.
- Dmitriev, I., E. Kashentseva, B. E. Rogers, V. Krasnykh, and D. T. Curiel. 2000. Ectodomain of coxsackievirus and adenovirus receptor genetically fused to epidermal growth factor mediates adenovirus targeting to epidermal growth factor receptor-positive cells. *J. Virol.* **74**:6875–6884.
- Dmitriev, I., V. Krasnykh, C. R. Miller, M. Wang, E. Kashentseva, G. Mikheeva, N. Belousova, and D. T. Curiel. 1998. An adenovirus vector with genetically modified fibers demonstrates expanded tropism via utilization of a coxsackievirus and adenovirus receptor-independent cell entry mechanism. *J. Virol.* **72**:9706–9713.
- Douglas, J. T., C. R. Miller, M. Kim, I. Dmitriev, G. Mikheeva, V. Krasnykh, and D. T. Curiel. 1999. A system for the propagation of adenoviral vectors with genetically modified receptor specificities. *Nat. Biotechnol.* **17**:470–475.
- Dveksler, G. S., C. W. Dieffenbach, C. B. Cardellichio, K. McCuaig, M. N. Pensiero, G.-S. Jiang, N. Beauchemin, and K. V. Holmes. 1993. Several members of the mouse carcinoembryonic antigen-related glycoprotein family are functional receptors for the coronavirus mouse hepatitis virus-A59. *J. Virol.* **67**:1–8.
- Dveksler, G. S., S. E. Gagneten, C. A. Scanga, C. B. Cardellichio, and K. V. Holmes. 1996. Expression of the recombinant anchorless N-terminal domain of mouse hepatitis virus (MHV) receptor makes hamster or human cells susceptible to MHV infection. *J. Virol.* **70**:4142–4145.
- Dveksler, G. S., M. N. Pensiero, C. B. Cardellichio, R. K. Williams, G. S. Jiang, K. V. Holmes, and C. W. Dieffenbach. 1991. Cloning of the mouse hepatitis virus (MHV) receptor: expression in human and hamster cell lines confers susceptibility to MHV. *J. Virol.* **65**:6881–6891.
- Dveksler, G. S., M. N. Pensiero, C. W. Dieffenbach, C. B. Cardellichio, A. A. Basile, P. E. Elia, and K. V. Holmes. 1993. Mouse hepatitis virus strain A59 and blocking antireceptor monoclonal antibody bind to the N-terminal domain of cellular receptor. *Proc. Natl. Acad. Sci. USA* **90**:1716–1720.
- Fuerst, T. R., E. G. Niles, F. W. Studier, and B. Moss. 1986. Eukaryotic transient-expression system based on recombinant vaccinia virus that synthesizes bacteriophage T7 RNA polymerase. *Proc. Natl. Acad. Sci. USA* **83**:8122–8126.
- Gagneten, S., O. Gout, M. Dubois-Dalcq, P. Rottier, J. Rossen, and K. V. Holmes. 1995. Interaction of mouse hepatitis virus (MHV) spike glycoprotein with receptor glycoprotein MHVR is required for infection with an MHV strain that expresses the hemagglutinin-esterase glycoprotein. *J. Virol.* **69**:889–895.
- Gallagher, T. M. 1997. A role for naturally occurring variation of the murine coronavirus spike protein in stabilizing association with the cellular receptor. *J. Virol.* **71**:3129–3137.
- Gallagher, T. M., M. J. Buchmeier, and S. Perlman. 1992. Cell receptor-independent infection by a neurotropic murine coronavirus. *Virology* **191**:517–522.
- Hallak, L. K., J. R. Merchan, C. M. Storgard, J. C. Loftus, and S. J. Russell. 2005. Targeted measles virus vector displaying echistatin infects endothelial cells via alpha(v)beta3 and leads to tumor regression. *Cancer Res.* **65**:5292–5300.
- Hammond, A. L., R. K. Plempner, J. Zhang, U. Schneider, S. J. Russell, and R. Cattaneo. 2001. Single-chain antibody displayed on a recombinant measles virus confers entry through the tumor-associated carcinoembryonic antigen. *J. Virol.* **75**:2087–2096.
- Hay, C. M., H. De Leon, J. D. Jafari, J. L. Jakubczak, C. A. Mech, P. L. Hallenbeck, S. K. Powell, G. Liau, and S. C. Stevenson. 2001. Enhanced gene transfer to rabbit jugular veins by an adenovirus containing a cyclic RGD motif in the HI loop of the fiber knob. *J. Vasc. Res.* **38**:315–323.
- Hemminki, A., M. Wang, T. Hakkarainen, R. A. Desmond, J. Wahlfors, and D. T. Curiel. 2003. Production of an EGFR targeting molecule from a conditionally replicating adenovirus impairs its oncolytic potential. *Cancer Gene Ther.* **10**:583–588.
- Katane, M., E. Takao, Y. Kubo, R. Fujita, and H. Amanuma. 2002. Factors affecting the direct targeting of murine leukemia virus vectors containing peptide ligands in the envelope protein. *EMBO Rep.* **3**:899–904.
- Kim, J., T. Smith, N. Idamakanti, K. Mulgrew, M. Kaloss, H. Kylefjord, P. C. Ryan, M. Kaleko, and S. C. Stevenson. 2002. Targeting adenoviral vectors by using the extracellular domain of the coxsackie-adenovirus receptor: improved potency via trimerization. *J. Virol.* **76**:1892–1903.
- Krasnykh, V., I. Dmitriev, G. Mikheeva, C. R. Miller, N. Belousova, and D. T. Curiel. 1998. Characterization of an adenovirus vector containing a heterologous peptide epitope in the HI loop of the fiber knob. *J. Virol.* **72**:1844–1852.
- Krasnykh, V. N., J. T. Douglas, and V. W. van Beusechem. 2000. Genetic targeting of adenoviral vectors. *Mol. Ther.* **1**:391–405.
- Kubo, H., Y. K. Yamada, and F. Taguchi. 1994. Localization of neutralizing epitopes and the receptor-binding site within the amino-terminal 330 amino acids of the murine coronavirus spike protein. *J. Virol.* **68**:5403–5410.
- Kuo, L., G. J. Godeke, M. J. Raamsman, C. R. Miller, and P. J. Rottier. 2000. Retargeting of coronavirus by substitution of the spike glycoprotein ectodomain: crossing the host cell species barrier. *J. Virol.* **74**:1393–1406.
- Lindner, P., K. Bauer, A. Krebber, L. Nieba, E. Kremmer, C. Krebber, A. Honegger, B. Klingler, R. Mockat, and A. Pluckthun. 1997. Specific detection of his-tagged proteins with recombinant anti-His tag scFv-phosphatase or scFv-phage fusions. *BioTechniques* **22**:140–149.
- Matsuyama, S., and F. Taguchi. 2002. Receptor-induced conformational changes of murine coronavirus spike protein. *J. Virol.* **76**:11819–11826.
- Michael, S. I., J. S. Hong, D. T. Curiel, and J. A. Engler. 1995. Addition of a short peptide ligand to the adenovirus fiber protein. *Gene Ther.* **2**:660–668.
- Miura, H. S., K. Nakagaki, and F. Taguchi. 2004. N-terminal domain of the murine coronavirus receptor CEACAM1 is responsible for fusogenic activation and conformational changes of the spike protein. *J. Virol.* **78**:216–223.
- Nakano, K., R. Asano, K. Tsumoto, H. Kwon, W. F. Goins, I. Kumagai, J. B. Cohen, and J. C. Glorioso. 2005. Herpes simplex virus targeting to the EGF receptor by a gD-specific soluble bridging molecule. *Mol. Ther.* **11**:617–626.
- Nedellec, P., G. S. Dveksler, E. Daniels, C. Turbide, B. Chow, A. A. Basile, K. V. Holmes, and N. Beauchemin. 1994. Bgp2, a new member of the carcinoembryonic antigen-related gene family, encodes an alternative receptor for mouse hepatitis viruses. *J. Virol.* **68**:4525–4537.
- Nicklin, S. A., and A. H. Baker. 2002. Tropism-modified adenoviral and adeno-associated viral vectors for gene therapy. *Curr. Gene Ther.* **2**:273–293.
- Ohtsuka, N., Y. K. Yamada, K. Saeki, and F. Taguchi. 1998. Differential receptor-functionality of the two distinct receptor proteins for mouse hepatitis virus. *Adv. Exp. Med. Biol.* **440**:77–80.
- Ohtsuka, N., Y. K. Yamada, and F. Taguchi. 1996. Difference in virus-binding activity of two distinct receptor proteins for mouse hepatitis virus. *J. Gen. Virol.* **77**:1683–1692.
- Peng, K. W., K. A. Donovan, U. Schneider, R. Cattaneo, J. A. Lust, and S. J. Russell. 2003. Oncolytic measles viruses displaying a single-chain antibody against CD38, a myeloma cell marker. *Blood* **101**:2557–2562.

37. Peng, K. W., and S. J. Russell. 1999. Viral vector targeting. *Curr. Opin. Biotechnol.* **10**:454–457.
38. Rao, P. V., and T. M. Gallagher. 1998. Mouse hepatitis virus receptor levels influence virus-induced cytopathology. *Adv. Exp. Med. Biol.* **440**:549–555.
39. Rao, P. V., S. Kumari, and T. M. Gallagher. 1997. Identification of a contiguous 6-residue determinant in the MHV receptor that controls the level of virion binding to cells. *Virology* **229**:336–348.
40. Ries, S. J., and C. H. Brandts. 2004. Oncolytic viruses for the treatment of cancer: current strategies and clinical trials. *Drug Discov. Today* **9**:759–768.
41. Rottier, P. J., M. C. Horzinek, and B. A. van der Zeijst. 1981. Viral protein synthesis in mouse hepatitis virus strain A59-infected cells: effect of tunicamycin. *J. Virol.* **40**:350–357.
42. Saeki, K., N. Ohtsuka, and F. Taguchi. 1998. Isolation and characterization of murine coronavirus mutants resistant to neutralization by soluble receptors. *Adv. Exp. Med. Biol.* **440**:11–16.
43. Schneider, U., F. Bullough, S. Vongpunsawad, S. J. Russell, and R. Cattaneo. 2000. Recombinant measles viruses efficiently entering cells through targeted receptors. *J. Virol.* **74**:9928–9936.
44. Shi, W., and J. S. Bartlett. 2003. RGD inclusion in VP3 provides adeno-associated virus type 2 (AAV2)-based vectors with a heparan sulfate-independent cell entry mechanism. *Mol. Ther.* **7**:515–525.
45. Stevenson, S. C., M. Rollence, J. Marshall-Neff, and A. McClelland. 1997. Selective targeting of human cells by a chimeric adenovirus vector containing a modified fiber protein. *J. Virol.* **71**:4782–4790.
46. Sturman, L. S., C. S. Ricard, and K. V. Holmes. 1985. Proteolytic cleavage of the E2 glycoprotein of murine coronavirus: activation of cell-fusing activity of virions by trypsin and separation of two different 90K cleavage fragments. *J. Virol.* **56**:904–911.
47. Taguchi, F., and S. Matsuyama. 2002. Soluble receptor potentiates receptor-independent infection by murine coronavirus. *J. Virol.* **76**:950–958.
48. Tan, K., B. D. Zelus, R. Meijers, J. H. Liu, J. M. Bergelson, N. Duke, R. Zhang, A. Joachimiak, K. V. Holmes, and J. H. Wang. 2002. Crystal structure of murine sCEACAM1a[1,4]: a coronavirus receptor in the CEA family. *EMBO J.* **21**:2076–2086.
49. Tsai, J. C., B. D. Zelus, K. V. Holmes, and S. R. Weiss. 2003. The N-terminal domain of the murine coronavirus spike glycoprotein determines the CEA CAM1 receptor specificity of the virus strain. *J. Virol.* **77**:841–850.
50. Vennema, H., L. Heijnen, A. Zijderveld, M. C. Horzinek, and W. J. Spaan. 1990. Intracellular transport of recombinant coronavirus spike proteins: implications for virus assembly. *J. Virol.* **64**:339–346.
51. Wessner, D. R., P. C. Shick, J. H. Lu, C. B. Cardellicchio, S. E. Gagneten, N. Beauchemin, K. V. Holmes, and G. S. Dveksler. 1998. Mutational analysis of the virus and monoclonal antibody binding sites in MHVR, the cellular receptor of the murine coronavirus mouse hepatitis virus strain A59. *J. Virol.* **72**:1941–1948.
52. Williams, R. K., G. S. Jiang, and K. V. Holmes. 1991. Receptor for mouse hepatitis virus is a member of the carcinoembryonic antigen family of glycoproteins. *Proc. Natl. Acad. Sci. USA* **88**:5533–5536.
53. Würdinger, T., M. H. Verheije, K. Broen, B. J. Bosch, B. J. Haijema, C. A. M. de Haan, V. W. van Beusechem, W. R. Gerritsen, and P. J. M. Rottier. 2005. Soluble receptor-mediated targeting of mouse hepatitis coronavirus to the human epidermal growth factor receptor. *J. Virol.* **79**:15314–15322.
54. Würdinger, T., M. H. Verheije, M. Raaben, B. J. Bosch, C. A. M. de Haan, V. W. van Beusechem, P. J. M. Rottier, and W. R. Gerritsen. 2005. Targeting non-human coronaviruses to human cancer cells using a bispecific single-chain antibody. *Gene Ther.* **12**:1394–1404.
55. Yokomori, K., and M. M. Lai. 1992. Mouse hepatitis virus utilizes two carcinoembryonic antigens as alternative receptors. *J. Virol.* **66**:6194–6199.
56. Zelus, B. D., J. H. Schickli, D. M. Blau, S. R. Weiss, and K. V. Holmes. 2003. Conformational changes in the spike glycoprotein of murine coronavirus are induced at 37°C either by soluble murine CEACAM1 receptors or by pH 8. *J. Virol.* **77**:830–840.
57. Zelus, B. D., D. R. Wessner, G. S. Dveksler, and K. V. Holmes. 1998. Neutralization of MHV-A59 by soluble recombinant receptor glycoproteins. *Adv. Exp. Med. Biol.* **440**:3–9.
58. Zelus, B. D., D. R. Wessner, R. K. Williams, M. N. Pensiero, F. T. Phibbs, M. deSouza, G. S. Dveksler, and K. V. Holmes. 1998. Purified, soluble recombinant mouse hepatitis virus receptor, Bgp1<sup>B</sup>, and Bgp2 murine coronavirus receptors differ in mouse hepatitis virus binding and neutralizing activities. *J. Virol.* **72**:7237–7244.